Dynamic Interfacial Mechanical-Thermal Characteristics of Atomically Thin Two-Dimensional Crystals

Kunqi Xu,[a] Shili Ye,[a, b, c] Le Lei,[b] Lan Meng,[d] Sabir Hussain,[a, c] Zhiyue Zheng,[a] Huarong Zeng,[e] Wei Ji,[b] Rui Xu*[a, b] and Zhihai Cheng*[b]

[a.] *CAS Key Laboratory of Standardization and Measurement for Nanotechnology, CAS Centre for Excellence in Nanoscience, National Centre for Nanoscience and Technology, Beijing 100190, People's Republic of China. E-mail: xur@nanoctr.cn*

[b.] *Beijing Key Laboratory of Optoelectronic Functional Materials & Micro-nano Devices, Department of Physics, Renmin University of China, Beijing 100872, People's Republic of China. E-mail: zhihaicheng@ruc.edu.cn*

[c.] *University of Chinese Academy of Sciences, Beijing 100039, People's Republic of China.*

[d.] *College of Electronic Science and Engineering, Nanjing University of Posts and Telecommunications, Nanjing 210046, China*

[e.] *Key Laboratory of Inorganic Functional Materials and Devices, Shanghai Institute of Ceramics, Chinese Academy of Sciences, Shanghai 200050, People's Republic of China*

Supplementary Information

1. Model and analysis for quantitative TR solution based on SThM

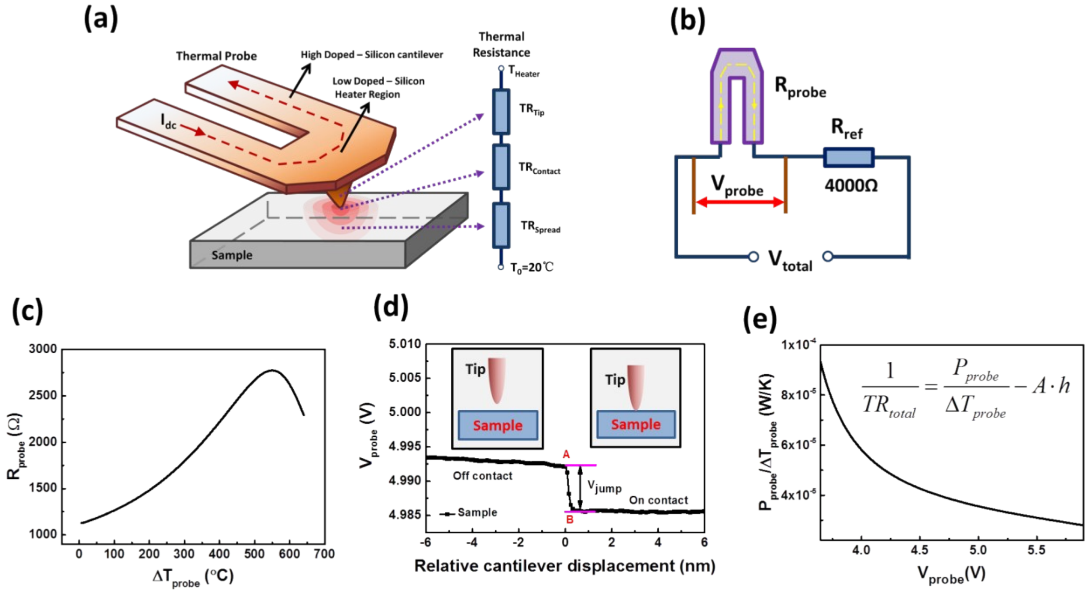

Figure S1. Supplementary Illustration of SThM. (a) The schematic diagram for the principle of thermal probe. **(b)** The circuit diagram of the local thermal analysis (ZThermal) module. **(c)** The curve of the probe electric resistance (R_{probe}) versus its temperature ($\Delta T_{probe} = T_{probe} - T_{air}$). **(d)** The demonstration of the thermal tip-sample approach curve. **(e)** The curve of thermal conductivity (the reciprocal of thermal resistance) versus tip voltage. Thermal conductivity (resistance) is negatively (positively) correlated with the probe voltage. The total voltage is applied with 15V.

As the description in this paper, it is the heater region integrated in the thermal probe that can be used to control and monitor the temperature change. So when the thermal tip contact the sample, the total thermal resistance (TR_{total}) that can be measured is the sum of thermal resistance of the tip (TR_{tip}), contact thermal resistance ($TR_{contact}$) and the thermal spreading resistance of the sample (TR_{sample}), seen in **Fig.S1a**. As the tip thermal resistance is a constant, the value of the total thermal resistance actually only contains the information of contact thermal resistance and the sample thermal resistance. So in this paper, we take the heater region and the tip as a whole and need not discriminate them. The ZThermal module circuit for thermal probe installation is described in **Fig.S1b**. In this circuit, only the electric resistance of the reference electrical resistor is known (R_{ref}=4000Ω), and the total voltage (V_{total}) and probe voltage (V_{probe}) can be exerted or detected. At the same time, the electric resistance of the probe is thermosensitive, and the relationship of the electric resistance (R_{probe}) versus temperature ($\Delta T_{probe} = T_{probe} - T_{air}$) is shown in **Fig.S1c**.

According to **Fig.S1c**, the temperature that maximum electric resistance corresponds to is 550℃. And below 550℃, every electric resistance of probe corresponds to a specific temperature, while the electric resistance of probe can be calculated as following expression.

$$R_{probe} = \frac{V_{probe}}{V_{total} - V_{probe}} R_{ref} \sim \Delta T_{probe} \tag{S1}$$

And the thermal power generated by the thermal probe can be calculated as following expression.

$$P_{probe} = \frac{V_{probe}{}^{2}}{R_{probe}} \tag{S2}$$

We introduce the design idea of null point scanning thermal microscopy [20] and the quantized thermal transport characterization [21] and use the thermal tip-sample approach curve to calculate the value of TR. A model was built. The model assumes at the moment of the tip abruptly upon contact, the thermal circumstance does not change, so the heat transfer coefficient (h) of the thermal tip in the air does not change. However, before contact, the heat ($Q_{air,off}$) generated by the thermal tip all dissipates into the air, while after contact, a new thermal flow channel is opened and a part of the heat (Q_{sample}) is diffused into the sample. The heat power generated by the thermal probe is divided into two parts ($Q_{air,on}$ and Q_{sample}), thus the heat transfer equation can be given as

Off contact: $$P_{off} = Q_{air,off} = A \cdot h \cdot \Delta T_{off} \tag{S3}$$

On contact: $$P_{on} = Q_{air,on} + Q_{sample} = A \cdot h \cdot \Delta T_{on} + \frac{1}{TR_{total}} \cdot \Delta T_{on} \tag{S4}$$

Where the A stands for the superficial area of the tip; P_{off} and P_{on} stand for the heat power generated by the thermal probe before and after contact, respectively. The total thermal resistance can be deduced from above, as following

$$\frac{1}{TR_{total}} = \frac{P_{on}}{\Delta T_{on}} - \frac{P_{off}}{\Delta T_{off}} \tag{S5}$$

Based on the thermal tip-sample approach curve (**Fig.S1d**), according to the tip voltages of point A and B, combined with the Eq.S1-S5, the total thermal resistance can be solved.

In this paper, we fix the total voltage of 15V, because the slope of the curve in **Fig.S1c** at such voltage is relative large so that the thermal response is more sensitive. Based on Eq.S4, an equation can deduced (seen in the inset of **Fig.S1e**) as following

$$\frac{1}{TR_{total}} = \frac{P_{on}}{\Delta T_{on}} - A \cdot h \tag{S6}$$

At the total voltage of 15V, the curve of thermal conductivity versus probe voltage in **Fig.S1e** shows that the thermal resistance is positively correlated with the probe voltage. Therefore, we use probe voltage to represent the thermal resistance signal.

2. SThM quantitative characterization and SThM imaging

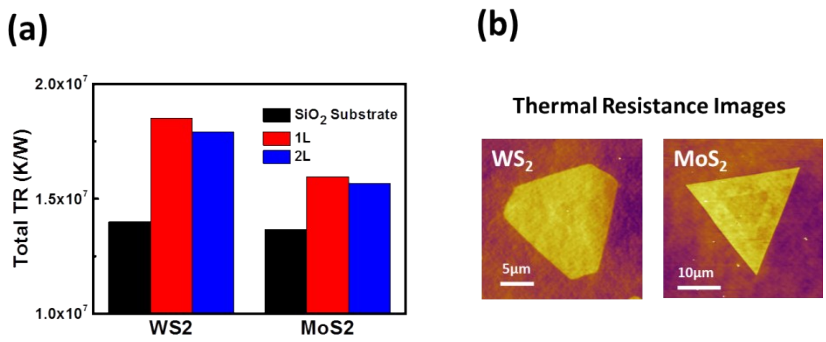

Figure S2. The SThM results of atomically thin MoS_2 and WS_2 epitaxially grown by chemical vapour deposition (CVD). (**a**) The histogram of the static thermal resistances of MoS_2 and WS_2. (**b**) SThM images (thermal resistance images) of MoS_2 and WS_2. The histogram and images are the results of in-situ SThM characterizations, corresponding to Fig.1b.

3. Absolute TR signals and relative TR signals

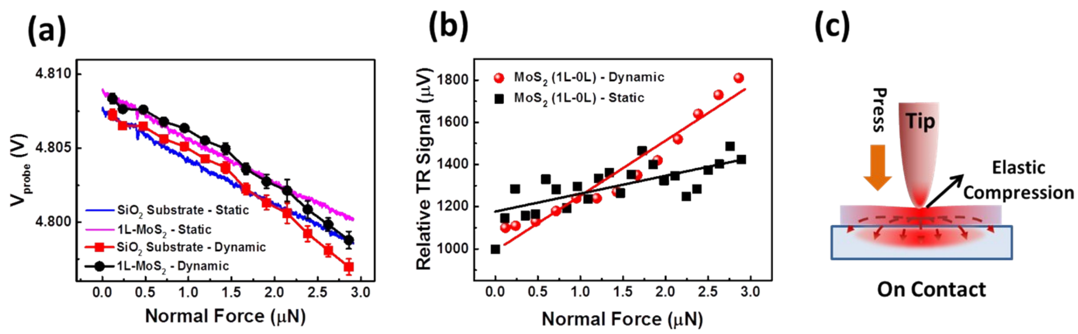

Figure S3. (**a**) The curves of the absolute dynamic/static thermal resistance signals (probe voltages) of the sample and the substrate versus normal forces. (**b**) The curves of the relative dynamic/static thermal resistance versus normal force. (**c**) The schematic diagram for thermal resistance under the normal force. With the increase of normal force, the larger elastic compression makes thermal contact area increased, companied with the decrease of TR.

This kind of thermal probe is extremely thermosensitive. When the total voltage is applied with 15V, the output voltage of the probe usually is about 5V, but the probe can monitor the voltage variation of tens of microvolts. So the probe voltage signal is easily disturbed by environmental conditions. **Fig.S3a** presents the curves of the absolute probe voltages versus normal forces. We can see the large disturbance of dynamic TR signals probably owing to the environmental instability or system signal drift. In fact, according to **Fig.S3b**, on the same scan condition, the difference value of the dynamic TR signals of the sample minus that of the substrate is very stable. Therefore in order to get a more reliable conclusion, we usually use relative value to analyse the problems.

At the same time, according to **Fig.3e**, the relative static TR is not sensitive to the normal force. In fact, according to **Fig.S3a**, the absolute TR signals decrease with the increase of normal force, which indicates that the larger normal force can lead to the enlargement of contact area owing to the elastic compression, resulting in the decrease of contact TR. But we infer that the elastic compression mainly is generated on the top layer between the thermal tip and the film instead of the interface layer between MoS_2 film and the SiO_2/Si substrate (**Fig.S3c**).

References:

1. K. Yoon, G. Hwang, J. Chung, H. G. Kim, O. Kwon, K. D. Kihm and J. S. Lee, *Carbon*, 2014, **76**, 77-83.
2. B. Gotsmann and M. A. Lantz, *Nat. Mater.*, 2013, **12**, 59-65.